Multi-User Entanglement Routing for Quantum Mesh Networks

Evan Sutcliffe[1]*, Matty J. Hoban[2], Alejandra Beghelli[1]

[1] *Optical Networks Group, Electronic & Electrical Engineering Department, University College London, London, WC1E 7JE, UK*

[2] *Cambridge Quantum Computing Ltd, 17 Beaumont St, Oxford OX1 2NA*

**evan.sutcliffe.20@ucl.ac.uk*

Abstract: Multipath routing for sharing entanglement between multiple devices was simulated on real network topologies and compared against single-path routing. Results show improved entanglement rates, especially for topologies with a higher average nodal degree. © 2022 The Author(s)

1. Introduction

Quantum networks allow quantum information, in the form of entanglement, to be shared over long distances and facilitate specific security and quantum computation applications [1]. However, quantum networks are challenging to implement, with low entanglement rates (ER), which decrease exponentially with distance. Previous work for bipartite entanglement has shown entanglement rates can be improved with multipath routing, which can utilise multiple potential paths through the network [2]. This approach has been simulated on grid topologies as well as some random graphs with known nodal degree distributions. An important task for quantum networks will be the distribution of multipartite states, which are required for certain secret sharing and distributed quantum computation applications [3]. We have shown that using multipath routing also gives an exponential speedup for distributing multipartite states over a quantum network [4]. However, the latter has only been demonstrated on regular grid topologies and the benefits of multipath routing might fade in real mesh networks. In this paper, we show that multipath routing provides a speedup over non-regular topologies, taken from classical optical networks. Further, we show how the entanglement rate achieved by the multipath protocol is dependent on the topology. Finally, the scaling of the multipath protocol with multipartite state size is examined.

2. Model and Assumptions

Quantum network. A quantum network can be described by a graph $G(V,E)$ of nodes V and edges E, such as seen in Figure 1. Edges represent channels over which *entanglement links*, which are $|\sigma^+\rangle = \frac{1}{\sqrt{2}}(|00\rangle + |11\rangle)$ states, are shared. For communication, entangled qubits can be encoded as single photons, and thus edges can be implemented using fiber optic channels or free space. In the graph nodes represent quantum devices, which can perform local qubit operations and classical communication (LOCC). This allows the nodes to perform entanglement swapping - to generate long-distance entanglement, or entanglement fusion - to create a multipartite state from multiple entanglement links [2]. Nodes are equipped with one quantum memory per connected edge.

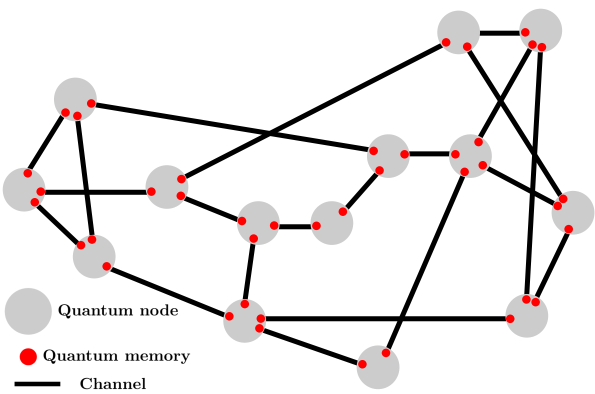

Fig. 1: A quantum network diagram (NSFnet).

Table 1: Real mesh optical networks from [5]

Network Name	Nodes	Edges	Average edge length (km)	Average nodal degree
ARPA	20	31	6.09	3.1
EON	20	39	7.24	3.9
Eurocore	11	25	4.26	4.55
NSFnet	14	21	5.09	3.0
UKnet	21	39	1.38	3.71
USnet	46	76	4.34	3.3
Grid	36	60	1.0	3.33

Temporal evolution and entanglement. The temporal evolution of the network was modelled as discrete timesteps of length T_{slot}. During each timestep, entanglement links are attempted, which are then used in LOCC operations to generate the shared multipartite state. If all the required entanglement links did not succeed, the protocol is reattempted the next timestep. It is assumed that the quantum memories are sufficient to store the qubits for only a single timestep, after which they must be used or are assumed to have undergone decoherence and discarded. Entanglement link generation is error-prone and hence probabilistic. The probability of successfully generating an entanglement link over an edge can be modelled using Eq (1).

$$p = p_{\text{op}}(1 - p_{\text{loss}}) \tag{1}$$

The value of p_{loss} is the probability of the photonic qubit being lost in the channel. We consider optical fiber of length L km and attenuation 0.2 dB/km, to have a probability of loss given by $p_{\text{loss}} = 10^{-0.2L/10}$. The operation probability p_{op} represents the lumped probability of successful entanglement between two back-to-back devices (e.g. at L = 0km). This accounts for errors and losses from multiple sub-operations, such as qubit-photon entanglement and photon frequency conversion. While current experimental values of p_{op} are of the order 10^{-4}, we consider p_{op} in the range $0-1$ [6]. This is justified as each timestep can represent multiple rounds of attempting entanglement links before routing, and the probability p_{op} represents that of successfully generating an entanglement link over an edge within a given timestep. Also, as the quantum memories are required to store the qubits of the entangled links, only a single entanglement link can be stored per timestep. For the network model, we assume that the entanglement distribution is heralded. That is, successful entanglement links are flagged by a classical signal. Further, when generating the multipartite state from entanglement links, we neglect the effect of qubit fidelity or errors during LOCC.

Multipartite routing protocols. Multipartite routing protocols aim to generate a multipartite state, shared between multiple users, which are nodes $S \in V$. We consider protocols which distribute N-qubit Greenberger–Horne–Zeilinger (GHZ) states, where $|GHZ\rangle_N = \frac{1}{\sqrt{2}}(|0\rangle^{\otimes N} + |1\rangle^{\otimes N})$ and $N = |S|$. We simulate network operation with the best performing multipartite multipath protocol known to date, MP-C [4]. The MP-C protocol attempts entanglement link generation on all edges in G. At the end of each timestep, routing is attempted using global link-state knowledge, in the form of the subgraph $G'(V,E')$ where edges represent entanglement links. The routing algorithm aims to find the minimum Steiner tree between users. The optimal routing solution is the minimum Steiner tree in G'. For multipartite states entanglement swapping and entanglement fusion are required to combine the shared entanglement links into a GHZ state. Entanglement fusion is performed at all nodes in the selected tree G' which have an edge degree (of entanglement links) greater than two.

3. Results

The MP-C protocol was evaluated using a Monte Carlo simulation. This was run on real-network topologies, which are described in Table 1, as well as a 6×6 square grid topology. The edge lengths were scaled down by a factor of 100. This was done to test the protocols on network topologies with channels that more closely match experimental systems [6]. The protocols were evaluated using the entanglement rate (ER) of GHZ states successfully distributed per timeslot GHZ_N/T_{slot}. The legend of Figure 2a also applies to later figures.

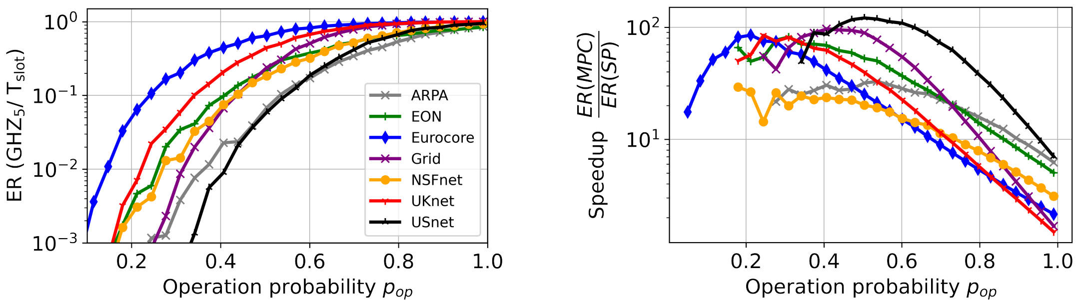

(a) (b)

Fig. 2: a) ER of MP-C with p_{op} for networks in Table 1. b) The speedup achieved by the MP-C protocol over SP for varied p_{op}. The probability of entanglement link generation over an edge is given by Eq. (1).

Figure 2a shows the ER for five randomly selected users. Datapoints represent 10^4 different user combinations, each attempted for up to 5000 timeslots. The ER was found with varied p_{op}, where Eq (1) gives the probability of entanglement link generation. For different networks, the ER followed similar trends but diverged for low p.

Despite a wide range of average edge lengths, topologies with high average node degrees such as Eurocore, EON and UKNet, achieved higher ERs. For the MP-C protocol, being able to utilise multiple possible paths means that a high nodal degree improves ER. Additionally, it was observed that the relationship between p_{op} and ER was not fixed, with different topologies performing better at different values of p_{op}.

The performance of the MP-C protocol was compared against the Shortest Path (SP) routing algorithm proposed in Bugalho *et al.* [3]. The tree-routing variant was selected, which attempts entanglement link generation over a specific tree in G. The tree selected is the minimum Steiner tree, found to maximise ER by minimising $\sum -log(p_i)$ for the ith edge in E. When all the required entanglement links have succeeded, the GHZ state is generated. Figure 2b shows the factor of improvement of MP-C over the SP protocol. Datapoints with MP-C below a ER = 10^-3 were excluding due to the effect of increasing model noise. The average speedup of the MP-C protocol was dependent on both topology and p_{op}. For the networks simulated a $25-135$ times maximum speedup was found, which was dependent on both the size of the network, as well as the average nodal degree. The maximum speedup occurred at intermediate values of p_{op}, which varied for different topologies. We hypothesised that multipath routing provides reduced benefit at high p, as the SP protocol is able to generate a GHZ state most timesteps. Further, for low p, any path longer than the minimum Steiner tree in G' will be unlikely to exist, reducing the benefit of multipath routing. There needs to be sufficiently high p for these possible longer paths to have a significant chance of existing.

The impact of the number of users on the ER achieved by the MP-C protocol was studied for distributing GHZ_N states for randomly selected users $N = |S|$. A benefit of the MP-C protocol is that a quantum centralised device is not required, and the size of the multipartite state distributed can scale freely with the number of users regardless of network topology. Figure 3 shows the ER for simulations run at a) $p_{op} = 0.5$ and b) $p_{op} = 0.7$. The ER decreases with the number of users, as larger trees are less likely to exist due to the probabilistic occurrence of entanglement links. The better performance of the Eurocore, UKnet and Grid networks was thought to be predominately due to their high nodal degree. The results also suggest there is a diminishing cost for each additional user. It was found that topologies have different ER-user relationships and that this relationship was not consistent with p_{op}, e.g. relative to the other topologies the Grid performed significantly better in Figure 3b than Figure 3a. This behaviour might be explained by the impact of p_{op} in the emergence of a large component in G'. Figure 3c shows the average size of the largest connected component (CC) in G'. All users being a part of the same CC is a sufficient condition for generating a GHZ state. The difference in the size of the CCs at $p_{op} = 0.5$ and $p_{op} = 0.7$ explains the ER scaling with the number of users for each network. Further work could develop expressions for the ER as a function of the network parameters directly using this relationship.

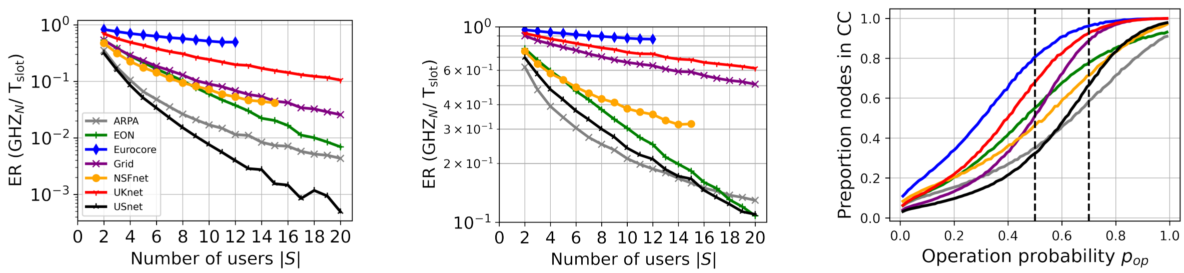

(a) (b) (c)

Fig. 3: ER of the MP-C protocol for the number of users $|S|$ at a) $p_{op} = 0.5$ and b) $p_{op} = 0.7$. c) average proportion of nodes which are part of the largest connected component in G'.

Acknowledgements: This work was supported by the Engineering and Physical Sciences Research Council [grant number EP/S021582/1].

References

1. S. Wehner et al, "Quantum internet: A vision for the road ahead," Science **362** (2018).
2. M. Pant et al, "Routing entanglement in the quantum internet," npj Quantum Inf. **5**, 1–9 (2019).
3. B Luís et al, "Distributing multipartite entanglement over noisy quantum networks," arXiv preprint arXiv:2103.14759 (2021).
4. E. Sutcliffe et al, "Multipath routing for multipartite state distribution in quantum networks," in *Quantum 2.0,* (Optica Publishing Group, 2022), pp. QTu2A–23.
5. S. Baroni, "Routing and wavelength allocation in WDM optical networks," https://discovery.ucl.ac.uk/id/eprint/10100693/1/Routing_and_wavelength_allocat.pdf (1998).
6. Y. Yu et al, "Entanglement of two quantum memories via fibres over dozens of kilometres," Nature **578**, 240–245 (2020).